Effect of pressure on crystal-field transitions of Nd-doped YVO₄

F. J. Manjón,[1,2,*] S. Jandl,[3] G. Riou,[3] B. Ferrand,[4] and K. Syassen[1]

[1]*Max-Planck-Institut für Festkörperforschung, Heisenbergstrasse 1, D-70569 Stuttgart, Germany*
[2]*Departament de Física Aplicada, Universitat Politècnica de València, EPSA, Pl. Ferrandiz i Carbonell, 2, E-03801 Alcoi, Spain*
[3]*Centre de Recherche sur les Propriétés Électroniques des Matériaux Avancés, Université de Sherbrooke, Sherbrooke,*
Québec J1K 2R1, Canada
[4]*LETI/DOPT/Laboratoire de Cristallogenèse Appliquée, CEA-Grenoble, 17 rue des Martyrs, F-38054 Grenoble Cedex 9, France*

The effect of hydrostatic pressure on crystal field (CF) transitions of Nd-doped YVO₄ has been studied by luminescence spectroscopy at $T = 5$ K. Specifically, emissions from the $^4F_{3/2}(1)$ and $^4F_{3/2}(2)$ excited levels to the $^4I_{9/2}$ and $^4I_{11/2}$ multiplets have been measured within the stability range of the zircon-type phase (7.5 GPa). The observed redshift of the emissions with increasing pressure is attributed to the decrease of the Slater free-ion and spin-orbit parameters and an increase of the CF interaction as pressure increases. Results obtained for CF parameters are compared to those of Nd^{3+} in YAsO₄ and YPO₄. Satellite lines observed in YVO₄:Nd can be assigned to Nd^{3+}-Nd^{3+} ion pairs coupled by ferromagnetic exchange interaction; the exchange coupling increases with pressure.

I. INTRODUCTION

Neodymium-doped yttrium orthovanadate (YVO₄:Nd³⁺) is used as laser-active material in diode-pumped microchip lasers. The Nd³⁺ ions have a strong absorption band around 0.81 μm and intense emission bands in the 1 and 1.3 μm range.[1] Continuous-wave visible laser emission in the three fundamental colors red, green, and blue has been reported using YVO₄:Nd³⁺ in combination with strontium-barium niobate nonlinear crystals; such systems are of interest for laser-based high brightness displays.[2]

In zircon-type YVO₄ and the isostructural compounds YPO₄ and YAsO₄, the Nd³⁺ ions show similar properties. The Y³⁺ host lattice ions, for which Nd³⁺ substitutes, are located in a D_{2d} site symmetry and are eightfold coordinated by oxygen. The tetragonal structure consists of chains of alternating edge-sharing YO₈ dodecahedra and MO₄ tetrahedra (M = V,P,As) running parallel to the c axis. Low-temperature luminescence spectra of Nd³⁺ crystal field (CF) transitions in doped YVO₄, YPO₄, and YAsO₄ single crystals have been reported and, using the overlap model,[3] the five nonzero CF Hamiltonian parameters (B_{20}, B_{40}, B_{44}, B_{60}, and B_{64}) have been calculated.[4]

A particular $^{2S+1}L_J$ state of the Nd³⁺ free ion on a D_{2d} site splits into a series of ($J + 1/2$) Kramers doublets (labeled 1,2,...) by the CF Hamiltonian. Hence, the CF interaction gives rise to five Stark levels (Kramers doublets) of the $^4I_{9/2}$ ground state, six levels of the $^4I_{11/2}$ excited state, and two levels for the $^4F_{3/2}$ state (see Fig. 1). In zircon-type YMO₄, changing M from V to P or As results in a reduction of the unit cell parameters, a decrease of the average Y-O distance, and changes in O-Y-O bond angles. This leads to marked changes in CF level energies and their corresponding CF parameters.[4]

High-resolution absorption and luminescence studies of YVO₄:Nd³⁺ have revealed satellites of the $^4F_{3/2}$–$^4I_{9/2}$ transitions, which depend on Nd³⁺ concentration. The satellites

are assigned to several types of ferromagnetically coupled Nd³⁺ pairs.[5] Zeeman effect studies have further confirmed lifting of the Kramers doublet degeneracies with various values of the exchange coupling J_i ranging from 0.8 to 4.9 cm⁻¹.[6,7] An interesting aspect of coupled-pair luminescence is that it may give rise to hysteresis and intrinsic bistability resulting from a cooperative effect due to ion-ion coupling within dimers.[8]

In YLiF₄:Nd³⁺, a scheelite compound with eight-coordinated Nd sites, the CF transitions have been studied recently as a function of hydrostatic pressure at $T = 5$ K.[9] Most of the isolated ion emissions show a red shift with increasing pressure resulting from a decrease of the Slater
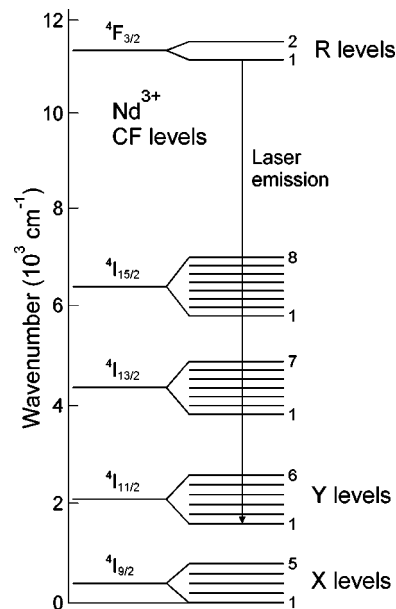

FIG. 1. Energy level diagram (schematic) of Nd³⁺ CF levels in the zircon-type structure of YVO₄. Stark levels are numbered in order of increasing energy.
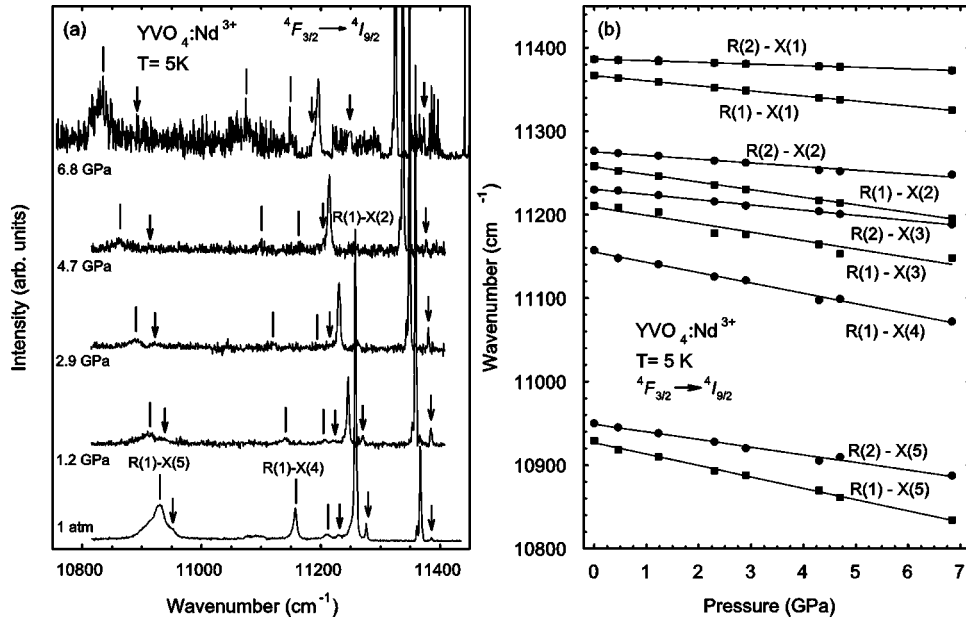
     69 165121-1

FIG. 2. (a) Low-temperature luminescence spectra of the $^4F_{3/2} \rightarrow {}^4I_{9/2}$ Nd^{3+} CF transitions in $YVO_4:Nd^{3+}$ at different pressures. Solid arrows and lines indicate the positions of $R(2)$ and $R(1)$ transitions of small intensity at different pressures respectively. Some parts of the spectrum at 6.8 GPa have been multiplied by a factor of five in order to show better the low intensity PL peaks. (b) Energies of the $^4F_{3/2} \rightarrow {}^4I_{9/2}$ CF transitions as a function of pressure.

free-ion and spin-orbit parameters and an increase of the CF interactions as pressure increases. Also, satellites of the $^4F_{3/2} \rightarrow {}^4I_{9/2}$ CF transition were observed; these indicated an increase of the ferromagnetic coupling of Nd^{3+}-Nd^{3+} pairs with pressure.

In this paper, we address the effect of the hydrostatic pressure on Nd^{3+} CF transitions in $YVO_4:Nd^{3+}$. High-pressure Raman studies of YVO_4 (Ref. 10) and of the Eu^{3+} emission in $YVO_4:Eu^{3+}$ (Ref. 11) indicate that the zircon-type phase (D_{4h}^{19}) is stable up to 7.5 GPa, where it transforms to a scheelite (C_{4h}^6) modification. Our aim here is to determine experimentally the evolution of the $^4F_{3/2} \rightarrow {}^4I_{9/2}$ and $^4F_{3/2} \rightarrow {}^4I_{11/2}$ CF transitions of Nd^{3+} in the zircon-type phase of YVO_4 with hydrostatic pressure, to compare with CF transitions in the structurally related but chemically different compounds $YAsO_4:Nd^{3+}$ and $YPO_4:Nd^{3+}$, and to determine the effect of pressure on the satellites originated by Nd^{3+}-Nd^{3+} pair coupling.

II. EXPERIMENTAL DETAILS

The YVO_4 crystals used in this study were single crystals with 0.58% Nd concentration grown by the Czochralski method. A single crystal sample (100 μm $\times$ 100 μm $\times$ 30 μm) was inserted in a diamond-anvil cell (DAC). Low-temperature measurements ($T=5$ K) were performed in a continuous-flow helium cryostat using the 5145 Å line of an Ar^+-ion laser for excitation of the Nd^{3+} ions luminescence. Helium was used as pressure transmitting medium to ensure hydrostatic conditions. Pressure changes were always performed above the helium melting temperature in order to prevent the built-up of nonhydrostatic stresses. The pressure was measured by the ruby luminescence method[12,13] using a temperature correction according to Ref. 14. The incident beam was parallel to the c axis and emitted light was analyzed by a 0.64 m focal length spectrometer equipped with a liquid-nitrogen-cooled Ge detector and a GaAs photomulti-

plier. Spectral resolutions were 1 cm^{-1} (100 μm slit width) in the 9400 cm^{-1} range and 0.3 cm^{-1} (20 μm slit width) in the 11400 cm^{-1} range. Argon plasma lines were used to calibrate the spectra.

III. RESULTS AND DISCUSSION

A. The $^4F_{3/2} \rightarrow {}^4I_{9/2}$ and $^4F_{3/2} \rightarrow {}^4I_{11/2}$ emissions

Figure 2(a) shows the luminescence spectra for the $^4F_{3/2} \rightarrow {}^4I_{9/2}$ transitions at different pressures. According to the level scheme (see Fig. 1) ten lines would be expected (assuming that the second Stark level of $^4F_{3/2}$ is populated at low temperatures). Nine peaks and their shifts with pressure were actually observed. In Fig. 2(b) we present the pressure dependence of the emission energies which, in accordance with Fig. 1, are denoted as $R(i)$-$X(j)$, $i=1,2$ and $j=1-5$. The missing band is assigned to the $R(2)$-$X(4)$ emission that corresponds to the $^4F_{3/2}(2) \rightarrow {}^4I_{9/2}(4)$ transition. In order to justify this assignment, we have performed additional temperature dependence PL measurements up to 150 K at ambient pressure. A new band around 11 175 cm^{-1}, 20 cm^{-1} above the $R(1)$-$X(4)$ emission, is detected above 15 K and attributed to the $R(2)$-$X(4)$ emission. Our assignments of the $R(1)$-$X(4)$ and $R(2)$-$X(4)$ bands are further supported by their evolution with the thermally increasing population of $^4F_{3/2}(2)$ at the expense of $^4F_{3/2}(1)$. Our assignment of the $R(1)$-$X(4)$ emission agrees with Refs. 15 and 16 but differs with Refs. 4, 17, 18, and 19 for which the $R(1)$-$X(4)$ emission band should be located around 11 135 cm^{-1}. All observed transitions show a red shift with increasing pressure. They can be separated into two groups according to their different pressure coefficients. Group 1 is formed by the $R(1)$-$X(j)$ lines, which show larger pressure coefficients than the $R(2)$-$X(j)$ lines, which form group 2. For each group of lines there is a common initial state, i.e., the $^4F_{3/2}(1)$ and $^4F_{3/2}(2)$ Kramers doublets. The $R(1)$-$X(1)$ and $R(2)$-$X(1)$ lines in Fig. 2(b) correspond to the pressure

TABLE I. Zero-pressure frequencies and frequency pressure coefficients of the isolated-ion $^4F_{3/2}\rightarrow^4I_{9/2}$ and $^4F_{3/2}\rightarrow^4I_{11/2}$ CF transitions in YVO_4:Nd^{3+} at 5 K. Energies of the $^4I_J(x)$ levels with respect to the ground state level $^4I_{9/2}(1)$ and corresponding pressure coefficients are listed in the lower part of the Table. Photoluminescence energies and linear pressure coefficients correspond to fits of peak maxima using equation $E(P)=E_0+a_1P$.

Transition	E_0 (cm^{-1})	a_1 (cm^{-1}/GPa)	Transition	E_0 (cm^{-1})	a_1 (cm^{-1}/GPa)
$^4F_{3/2}(2)\rightarrow^4I_{9/2}(1)$	11386.37(5)	$-1.98(7)$	$^4F_{3/2}(2)\rightarrow^4I_{11/2}(1)$	9419.04(4)	$-2.39(8)$
$^4F_{3/2}(1)\rightarrow^4I_{9/2}(1)$	11366.80(1)	$-6.06(5)$	$^4F_{3/2}(1)\rightarrow^4I_{11/2}(1)$	9399.76(1)	$-6.44(6)$
$^4F_{3/2}(2)\rightarrow^4I_{9/2}(2)$	11275.12(4)	$-4.37(6)$	$^4F_{3/2}(2)\rightarrow^4I_{11/2}(2)$	9399.00(4)	$-2.70(8)$
$^4F_{3/2}(1)\rightarrow^4I_{9/2}(2)$	11257.09(2)	$-9.08(3)$	$^4F_{3/2}(1)\rightarrow^4I_{11/2}(2)$	9378.80(2)	$-6.43(6)$
$^4F_{3/2}(2)\rightarrow^4I_{9/2}(3)$	11230.43(8)	$-6.24(5)$	$^4F_{3/2}(2)\rightarrow^4I_{11/2}(3)$	9338.13(8)	$-6.53(5)$
$^4F_{3/2}(1)\rightarrow^4I_{9/2}(3)$	11209.24(7)	$-10.07(2)$	$^4F_{3/2}(1)\rightarrow^4I_{11/2}(3)$	9318.81(3)	$-10.56(3)$
$^4F_{3/2}(2)\rightarrow^4I_{9/2}(4)$	11175.22(9)	$-$	$^4F_{3/2}(2)\rightarrow^4I_{11/2}(4)$	9318.00(9)	$-6.46(5)$
$^4F_{3/2}(1)\rightarrow^4I_{9/2}(4)$	11155.38(3)	$-12.39(1)$	$^4F_{3/2}(1)\rightarrow^4I_{11/2}(4)$	9304.68(5)	$-11.84(2)$
$^4F_{3/2}(2)\rightarrow^4I_{9/2}(5)$	10948.89(7)	$-9.15(2)$	$^4F_{3/2}(2)\rightarrow^4I_{11/2}(5)$	9230.04(7)	$-7.06(6)$
$^4F_{3/2}(1)\rightarrow^4I_{9/2}(5)$	10926.62(6)	$-13.59(1)$	$^4F_{3/2}(1)\rightarrow^4I_{11/2}(5)$	9211.27(6)	$-11.48(3)$
			$^4F_{3/2}(2)\rightarrow^4I_{11/2}(6)$	9203.80(8)	$-6.23(6)$
			$F_{3/2}(1)\rightarrow I_{11/2}(6)$	9184.41(6)	$-10.65(4)$

Kramers Doublet	$E_0(^4I_J)$ (cm^{-1})	a_1 (cm^{-1}/GPa)	Kramers Doublet	$E_0(^4I_J)$ (cm^{-1})	a_1 (cm^{-1}/GPa)
$^4I_{9/2}(1)$	0	0	$^4I_{11/2}(1)$	1967.04(5)	0.39(4)
$^4I_{9/2}(2)$	109.73(6)	3.03(8)	$^4I_{11/2}(2)$	1987.67(6)	0.50(4)
$^4I_{9/2}(3)$	155.85(10)	4.28(7)	$^4I_{11/2}(3)$	2047.64(7)	4.49(2)
$^4I_{9/2}(4)$	210.99(8)	6.35(6)	$^4I_{11/2}(4)$	2063.71(9)	5.46(1)
$^4I_{9/2}(5)$	438.59(9)	7.37(6)	$^4I_{11/2}(5)$	2155.18(8)	5.41(2)
			$^4I_{11/2}(6)$	2182.20(9)	4.43(3)

dependence of the $^4F_{3/2}(1)$ and the $^4F_{3/2}(2)$ doublets, respectively, relative to the ground state level $^4I_{9/2}(1)$. Our assignment of the $R(1)$-$X(4)$ and $R(2)$-$X(4)$ is further supported by the pressure dependence found for the measured $R(1)$-$X(4)$ emission, as can be observed in Table I.

Figure 3(a) shows the luminescence spectra of the $^4F_{3/2}$ $\rightarrow^4I_{11/2}$ transitions at different pressures. Twelve lines are expected and observed in this case. In Fig. 3(b) we present

the pressure dependence of the corresponding energies, denoted as $R(i)$-$Y(j)$, $i=1,2$ and $j=1-6$. Again, all bands show a red shift with increasing pressure, and all lines can be separated into two groups according to their different pressure coefficients.

The observed ambient pressure energies and pressure coefficients of the $^4F_{3/2}\rightarrow^4I_{9/2}$ and $^4F_{3/2}\rightarrow^4I_{11/2}$ transitions are summarized in Table I. The zero-pressure frequencies and the pressure coefficients of all the $^4I_J(n)$ CF levels with $J=9/2$ and $11/2$, measured relative to the ground state, are
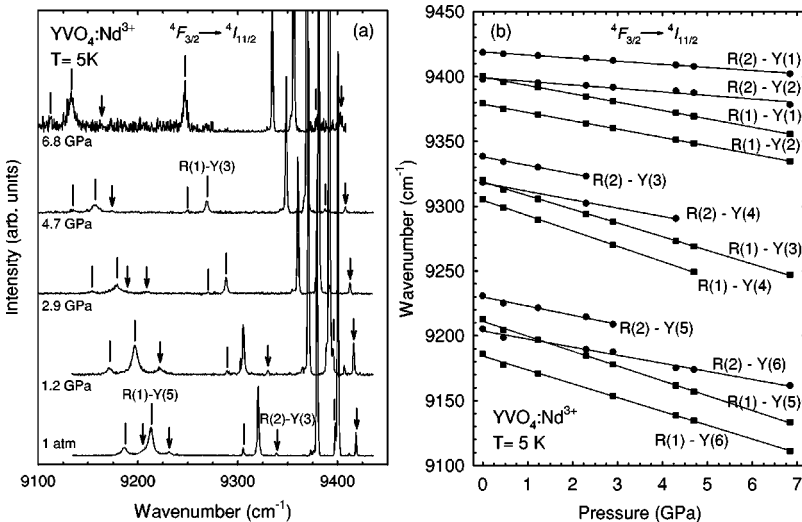

FIG. 3. (a) Low-temperature luminescence spectra of the $^4F_{3/2}\rightarrow^4I_{11/2}$ Nd^{3+} CF transitions in YVO_4:Nd^{3+} at different pressures. Solid arrows and lines indicate the positions of $R(2)$ and $R(1)$ transitions of small intensity at different pressures respectively. (b) Energies of the $^4F_{3/2}\rightarrow^4I_{11/2}$ CF transitions as a function of pressure.

TABLE II. Nd^{3+} ion crystal-field parameters (in cm^{-1}) of YVO_4 at different pressures and of $YAsO_4$ and YPO_4 at ambient pressure. Results are obtained by fitting the parameters of Eq. (1) to experimental data.

YVO_4	B_{20}	B_{40}	B_{44}	B_{60}	B_{64}
0 GPa	-158	463	-1110	-1170	300
1 GPa	-195	465	-1130	-1200	295
2 GPa	-230	469	-1150	-1230	283
3 GPa	-265	468	-1170	-1250	276
4 GPa	-297	470	-1190	-1280	270
5 GPa	-325	472	-1210	-1300	262
6 GPa	-351	461	-1240	-1330	254
7 GPa	-377	467	-1260	-1350	250
$YAsO_4$	-102	203	-951	-1060	-18
YPO_4	394	178	-725	-1301	-67

also given in Table I. All our results for the zero-pressure frequencies compare well with the previously reported experimental and calculated values at low temperature.[4]

The overall redshift of all $^4F_{3/2} \rightarrow {}^4I_{9/2}$ and $^4F_{3/2} \rightarrow {}^4I_{11/2}$ CF transitions with increasing pressure can basically be attributed to an increase of the covalency. Further, the smaller is the $^4F_{3/2}(1) \rightarrow {}^4I_J$ (n) transition energy for a given J the larger is the redshift observed; the latter effect is mainly related to the increase in the CF field interaction as pressure increases. A similar behavior has been observed for Nd^{3+} in $YLiF_4$ (Ref. 9) or Tm^{3+} (Ref. 20) and Cr^{3+} in YAG.[21]

The pressure coefficients for the emission energies in YVO_4 are almost twice the values found for the corresponding transitions in $YLiF_4$. The larger pressure dependences for the $^4F_{3/2}(1) \rightarrow {}^4I_{9/2}$ and $^4F_{3/2}(1) \rightarrow {}^4I_{11/2}$ transitions in YVO_4 as compared to $YLiF_4$ simply originates from the different pressure behavior of the $^4F_{3/2}(1)$ level. The values of the pressure coefficients for the Stark levels ^4I_J (n) are of similar magnitude in the two compounds for both the $^4I_{9/2}$ and $^4I_{11/2}$ levels.

In general, larger shifts of the transition frequencies are expected for the more compressible materials, i.e., with smaller bulk moduli.[22] The bulk modulus of YVO_4 is not known well but its value can be estimated by comparison to $DyVO_4$ to be about 160 GPa,[23] as compared to only 80 GPa for $YLiF_4$.[24] This means the pressure coefficients do not scale with compressibility of the two materials. Therefore, we think that the very small pressure coefficient of the $^4F_{3/2}(1)$ level in $YLiF_4$ as compared to the pressure coefficients of the $^4F_{3/2}$ levels in YVO_4, could indicate a near cancellation of pressure effects on the Slater free-ion parameters, spin-orbit parameters, and crystal field strength affecting the $^4F_{3/2}$ Stark levels in $YLiF_4$, which seems not to occur in YVO_4.

B. Fit of the CF Hamiltonian

In order to gain more insight in the physics underlying the behavior of the crystal field effects in $YVO_4:Nd^{3+}$, we have fitted the experimentally measured $^4I_{9/2}$ and $^4I_{11/2}$ CF levels to the CF Hamiltonian in the weak field limit, written in terms of one-electron irreducible tensor operators[25–27]

$$H_{CF} = \sum_{i,k,q} B_{kq} C_q^k(i). \qquad (1)$$

Here, $C_q^k(i)$ represents the qth component of a spherical tensor operator of rank k, and B_{kq} the corresponding CF parameter. In tetragonal symmetry, only five CF parameters B_{20}, B_{40}, B_{44}, B_{60}, and B_{64}, are nonzero. In order to calculate these values at different pressures, we have determined the barycenter energies of the $^{2S+1}L_J$ multiplets in an intermediate coupling scheme at each pressure and afterwards we have calculated the perturbations of these energies by the crystal field. In our calculation, we have diagonalized the matrix of the operator (H_{CF}) within the ^4I: 9/2, 11/2, 13/2, 15/2 multiplets including their J mixing. Since our measurements were restricted to the 9/2 and 11/2 levels, their free-ion energies were allowed to vary while those of the 13/2 and 15/2 levels were kept fixed in the fitting process. Even though the J mixing was limited in our calculations to the ^4I term and did not include higher energy terms, the overall predicted variation under pressure of the CF parameters should not be significantly affected.[28] Also, the CF parameters were determined by solving numerically the inverse secular problem with the initial values taken from Ref. 4. Explicit variation, as a function of pressure, of the free ion electrostatic parameters could not be accounted for in our procedure. Actually, many more level evolutions under pressure are required to describe a Hamiltonian that includes the centers of gravity of the multiplets and the CF splittings. Nevertheless, the frequency redshift with increasing pressure of the detected levels center of gravity reflects the nephelauxetic effect and its corresponding reduction of the Slater and spin-orbit coupling parameters.[29]

Table II summarizes the best fit results for different pressures. The measured Nd^{3+} CF energies compare well with the calculated energies. This is demonstrated in Fig. 4. The B_{20} parameter is the most sensitive one to a change in pressure, indicating that long-range electrostatic interactions are quite sensitive to pressure. Unfortunately, the lack of high-pressure structural data for YVO_4 prevents the *ab initio* calculation of the B_{20} parameter and the use of the superposi-
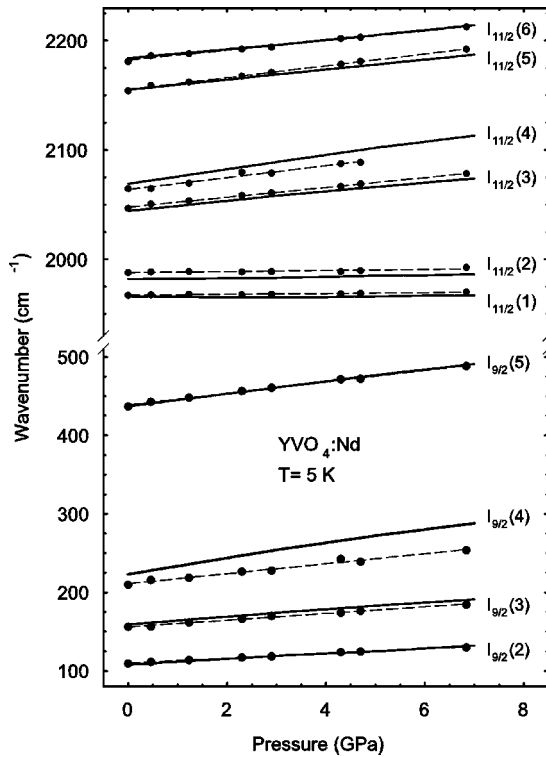
FIG. 4. Evolution of the $^4I_{9/2}$ and $^4I_{11/2}$ multiplet levels of Nd^{3+} in YVO_4 as a function of pressure. Experimental data are represented by symbols (thin dashed lines) and calculated results by solid lines.

tion model[27] for the evaluation of the other CF parameters, as was recently carried out in the case of Nd_2CuO_4.[30]

The calculated B_{kq} parameters allow us to obtain information about the evolution of the crystal field strength S experienced by the Nd^{3+} ion with increasing pressure. For that purpose we have used the following relationship:[31]

$$S = \left[\frac{1}{3} \sum_k \frac{1}{2k+1} \left(B_{k0}^2 + 2 \sum_{q>0} |B_{kq}|^2 \right) \right]^{1/2}. \quad (2)$$

The deduced Nd^{3+} CF strength in YVO_4 is 375 cm^{-1} at zero pressure and increases to 430 cm^{-1} at 6.8 GPa. The relative change of about 15%, when normalized to the estimated volume change of -5% at 6.8 GPa, corresponds to a volume scaling coefficient d ln S/d ln $V = -3$.

It could be expected that the Nd^{3+} CF values in YVO_4 under applied pressure approach those of $YAsO_4$ and YPO_4 which both have smaller average Y-O distances and smaller unit cell volumes (for $YAsO_4$ $a = 7.044$ Å, $c = 6.248$ Å; for YPO_4 $a = 6.888$ Å, $c = 6.021$ Å; for YVO_4 $a = 7.119$ Å, $c = 6.289$ Å). In order to compare the effect of the hydrostatic pressure and of the composition-induced variation of lattice parameters on the CF parameters, we have calculated the zero-pressure values of Nd^{3+} CF parameters in $YAsO_4$:Nd^{3+} and YPO_4:Nd^{3+}. For that purpose, and to assure comparison with YVO_4:Nd^{3+}, we have again used the two lowest experimentally measured $^4I_{9/2}$ and $^4I_{11/2}$ multiplet energies[4] for fitting. For both compounds, the experimentally observed Nd^{3+} CF levels are well reproduced by the CF

parameters obtained from Eq. (1) and given in Table II. The CF parameters essentially agree with those previously reported.[4] They seem to be extremely sensitive to the local environment as confirmed by the variations of the parallel and perpendicular g factors.[4,32]

Obviously, the evolution under pressure of the Nd^{3+} CF parameters in YVO_4 does not tend towards the $YAsO_4$:Nd^{3+} or YPO_4:Nd^{3+} parameters. Our results suggest that volume changes due to pressure and chemical composition affect CF parameters differently in the case of the zircon structure, in contrast to what is observed for spinel- and garnet-type hosts.[33] The difference between the three compounds is manifest if we compare the calculated crystal field strengths in YVO_4 and $YAsO_4$ and YPO_4 at zero pressure and compare the evolution of the crystal field strength with increasing pressure. The calculation with data from Table II yields a crystal field strength, at zero pressure, of 313 and 306 cm^{-1} for $YAsO_4$ and YPO_4, respectively. These values are comparable to those calculated from previously determined CF parameters.[4] Despite the shorter average Y-O distances in $YAsO_4$ (2.248–2.26 Å) and YPO_4 (2.30–2.37 Å) compared to YVO_4 (2.29–2.43 Å), their CF strengths are smaller and the difference increases further when YVO_4 is compressed. The origin of this apparent discrepancy could be of electrostatic or covalent nature. Screening effects and localization of $4f$ states are possibly modified by differences in chemical composition at sites outside of the first coordination shell.[34]

C. Satellites

At zero pressure, the luminescence spectrum of the $^4F_{3/2}(1) \rightarrow {}^4I_{9/2}(1)$ (ground state) transition consists of a central band at 11 366.80 cm^{-1} (the isolated-ion emission) and satellites which have been attributed to different types of ferromagnetically coupled Nd^{3+}-Nd^{3+} pairs with exchange coupling values $J_1 = 0.8$ cm^{-1}, $J_2 = 1.6$ cm^{-1}, $J_3 = 2.7$ cm^{-1}, and $J_4 = 4.9$ cm^{-1}.[5] For each ground-state exchange-coupled pair, a doublet of lines is expected at energies $E + J_i/2$ and $E - 3J_i/2$, where E refers to the isolated-ion transition and $J_i > 0$ represents a ferromagnetic Nd^{3+}-Nd^{3+} pair exchange energy.

In Fig. 5(a) we show an expanded view of the $^4F_{3/2}(1) \rightarrow {}^4I_{9/2}(1)$ luminescence of YVO_4:Nd^{3+} at several pressures. The spectra are shifted in energy such as to line up at the isolated-ion emission. The satellite energies reported in Ref. 5 are indicated by arrows and vertical bars placed near the horizontal axis.

On the various features seen in the spectra of Fig. 5(a) we comment as follows: (1) The band marked "site 2" is attributed to a different Nd^{3+} site. This is in agreement with previous Zeeman effect experiments[6] and with selective laser excitation and emission experiments.[35] Both experiments show that there are at least three types of Nd^{3+} sites in YVO_4, with one emission at the position expected for the "3/2 J_4" satellite. (2) The band marked by a question mark was not observed in previous luminescence studies. We do not rule out that it is a pair-interaction satellite of the main line, but its rather large pressure shift (relative to the main line) may point to a different origin. (3) Very clearly, a small
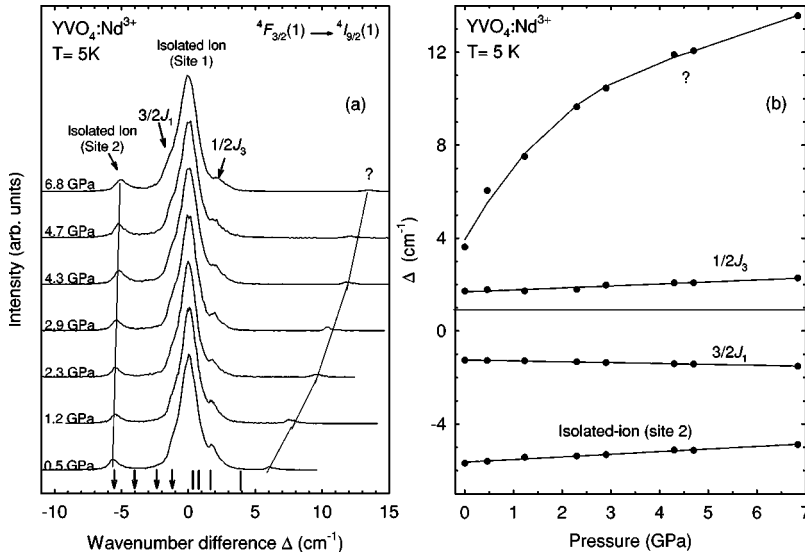
FIG. 5. (a) Expanded plots of luminescence spectra near the isolated-ion $^4F_{3/2}(1) \rightarrow {}^4I_{9/2}(1)$ transition in $YVO_4:Nd^{3+}$ at different pressures. The spectra have been shifted so as to align at the isolated-ion emission line. Lines and arrows mark the positions of the "$1/2\,J_i$" and "$3/2\,J_i$" satellites, respectively, at zero pressure. (b) Pressure dependence of the satellite energies corresponding to the $^4F_{3/2}(1) \rightarrow {}^4I_{9/2}(1)$ Nd^{3+} CF transition with respect to the isolated-ion emission.

peak on the high frequency side of the main line coincides with a spectral feature which was attributed to the "$1/2\,J_3$" satellite in Ref. 5. (4) Similarly, the shoulder on the low-frequency side of the main line appears to be related to the "$3/2\,J_1$" satellite. The shoulder is sufficiently pronounced such that the energy of the underlying peak can be determined through deconvolution. (5) The "$3/2\,J_2$" and "$3/2\,J_3$" satellites are not clearly observed in our spectra, and the evolution of the "$3/2\,J_4$" satellite is masked by the "site 2" band. (6) The "$1/2\,J_1$" and "$1/2\,J_2$" satellites are not resolved here because of overlap with the main line and limited resolution. Their pressure shift may contribute to the apparent broadening of the main line with increasing pressure.

In Fig. 5(b) we show the energies of the various side bands (measured relative to the isolated ion emission and denoted Δ in the following) as a function of pressure. The numerical values of the side band frequencies at ambient pressure and their pressure coefficients are listed in Table III. The splitting between the two assigned satellites and the isolated-ion emission increases with pressure. This behavior is similar to that found in Nd-doped $YLiF_4$.[11] At ambient pressure, the coupling between Nd^{3+} ion pairs is ferromagnetic and the increase of the energy splittings with pressure indicates that this coupling is significantly enhanced under pressure. The positive character of dJ_i/dP for the "$3/2\,J_1$" and "$1/2\,J_3$" satellites indicates that the ferromagnetic coupling between the Nd^{3+} ions conserves its character under pressure. This means that the distances of the Nd^{3+}-Nd^{3+} coupled ions responsible for these satellites are kept in the whole pressure range above the minimum value required for ferromagnetic exchange integrals.

If the unidentified side band in YVO_4 would originate from magnetically coupled ion pairs, it would indicate a nonlinear increase of the corresponding exchange coupling with increasing pressure. This could be related to a resonance effect in the Nd^{3+}-Nd^{3+} distance responsible for this satellite (with the rapid increase of the ferromagnetic exchange integrals close to the maximum).

Finally, we turn to the $^4F_{3/2}(1) \rightarrow {}^4I_{11/2}(1)$ CF transition in YVO_4. This transition is located at 9399.76 cm^{-1} (1064 nm) at ambient pressure and is one of the main laser lines in Nd-doped YVO_4. Two additional bands near the laser emission line were observed, at all pressures, on both sides of the isolated-ion line as in $YLiF_4$. Related information is collected in Table III. These bands reflect the Nd^{3+}-Nd^{3+} exchange interaction on the excited CF multiplet that was not considered in the ferromagnetic exchange interaction model of Ref. 4. On the basis of the energy splittings of these satellite lines, it can be assumed that both satellites correspond to the same doublet with $J_2 = 1.6$ cm^{-1}. These two satellites show an increase of the energy splitting with respect to the isolated-ion line as pressure increases, similarly to the $^4F_{3/2}(1) \rightarrow {}^4I_{9/2}(1)$ CF satellites.

TABLE III. Zero-pressure splittings Δ_0 and pressure coefficients of the side bands related to the isolated-ion emission of the $^4F_{3/2}(1) \rightarrow {}^4I_{9/2}(1)$ and $^4F_{3/2}(1) \rightarrow {}^4I_{11/2}(1)$ CF transitions.

Emission	Δ_0 (cm^{-1})	$d\Delta/dP$ (cm^1/GPa)
Not assigned[a]	3.94(3)	3.71(9)
$1/2\,J_3$	1.69(3)	0.09(1)
$1/2\,J_2$	Not resolved	
$1/2\,J_1$	Not resolved	
$^4F_{3/2}(1) \rightarrow {}^4I_{9/2}(1)$	0	0
$3/2\,J_1$	−1.24(5)	−0.04(1)
$3/2\,J_2$	Not observed	
$3/2\,J_3$	Not observed	
$^4F_{3/2}(1) \rightarrow {}^4I_{9/2}(1)$[b]	−5.64(3)	0.11(2)
HE	0.9(4)	0.01(1)
$^4F_{3/2}(1) \rightarrow {}^4I_{11/2}(1)$	0	0
LE	−2.26(4)	−0.06(2)

[a]The nonlinear behavior of this satellite follows the relation $E(P) = E(0) - 2.98P - 0.53P^2 - 0.04P^3$.

[b]This peak corresponds to the isolated ion emission from a secondary site (see text).

IV. CONCLUSIONS

We have investigated the effect of pressure on the $^4F_{3/2}$ $\to^4I_{9/2}$ and the $^4F_{3/2}\to^4I_{11/2}$ emissions of Nd^{3+} in zircon-type YVO_4, with some emphasis on the $^4F_{3/2}(1)$ $\to^4I_{11/2}(1)$ laser transition and on the satellites of the $^4F_{3/2}(1)\to^4I_{9/2}(1)$ transition. Our results show that chemical composition and hydrostatic pressures affect differently the CF parameters in the case of the zircon structure, which is in contrast to the spinels and garnets. We find that the increase of the crystal field interaction with pressure is similar in YVO_4:Nd^{3+} and $YLiF_4$:Nd^{3+}. The larger pressure coefficients for photoluminescence transitions in YVO_4 as compared to those of $YLiF_4$ can be attributed to a larger decrease of the Slater and spin-orbit parameters, which may be related to a stronger increase of the covalency with increasing pressure on the oxide compound. Regarding the satellites, their behavior indicates a significant increase of the Nd^{3+}-Nd^{3+} ferromagnetic exchange interaction as the distance between the pairs decreases. We have also observed a splitting of the $^4F_{3/2}(1)$ multiplet as a result of the Nd^{3+}-Nd^{3+} pairs exchange interaction.

*Electronic mail: fjmanjon@fis.upv.es

[1] D. G. Matthews, J. R. Boon, R. S. Conroy, and B. D. Sinclair, J. Mod. Opt. **43**, 1079 (1996).

[2] J. J. Romero, D. Jaque, J. García-Solé, and A. A. Kaminskii, Appl. Phys. Lett. **81**, 4106 (2002).

[3] O. L. Malta, Chem. Phys. Lett. **88**, 353 (1982).

[4] O. Guillot-Noël, A. Kahn-Harari, B. Viana, D. Vivien, E. Antic-Fidancev, and P. Porcher, J. Phys.: Condens. Matter **10**, 6491 (1998).

[5] O. Guillot-Noël, V. Mehta, B. Viana, D. Gourier, M. Boukhris, and S. Jandl, Phys. Rev. B **61**, 15 338 (2000).

[6] V. Mehta, O. Guillot-Noël, D. Gourier, Z. Ichalalène, M. Castonguay, and S. Jandl, J. Phys.: Condens. Matter **12**, 7149 (2000).

[7] S. Jandl, O. Guillot-Noël, and D. Gourier, Opt. Mater. (Amsterdam, Neth.) **19**, 449 (2002).

[8] C. M. Bowden and C. C. Sung, Phys. Rev. A **19**, 2392 (1979).

[9] F. J. Manjón, S. Jandl, K. Syassen, and J. Y. Gesland, Phys. Rev. B **64**, 235108 (2001).

[10] A. Jayaraman, G. A. Kourouklis, G. P. Espinosa, A. S. Cooper, and L. G. Van Uitert, J. Phys. Chem. Solids **48**, 755 (1987).

[11] G. Chen, N. A. Stump, R. G. Haire, J. R. Peterson, and M. M. Abrahams, J. Phys. Chem. Solids **53**, 1253 (1992).

[12] G. J. Piermarini, S. Block, J. D. Barnett, and R. A. Forman, J. Appl. Phys. **46**, 2774 (1975).

[13] H. K. Mao, J. Xu, and P. M. Bell, J. Geophys. Res. **91**, 4673 (1986).

[14] S. Buchsbaum, R. L. Mills, and D. Schiferl, J. Phys. Chem. **88**, 2522 (1984).

[15] R. J. Pressley, P. V. Foedertier, and H. Weakliem (unpublished).

[16] P. P. Yaney and L. G. DeShazer, J. Opt. Soc. Am. **66**, 1405 (1976).

[17] Kh. S. Bagdasarov, G. A. Bogomolova, A. A. Kaminskii, and V. I. Popov, Dokl. Akad. Nauk SSSR 180, 1347 (1968) [Sov. Phys. Dokl. **13**, 516 (1968)].

[18] N. Karayianis, C. Morrison, and D. E. Wortman, J. Chem. Phys. **62**, 4125 (1975).

[19] D. K. Sardar and R. M. Yow, Opt. Mater. (Amsterdam, Neth.) **14**, 5 (2000).

[20] P. R. Wamsley and K. L. Bray, J. Lumin. **60&61**, 188 (1994).

[21] Y. R. Shen and K. L. Bray, Phys. Rev. B **56**, 10 882 (1997).

[22] K. L. Bray, in *Transition Metal and Rare Earth Compounds, Vol. 213 of Topics in Current Chemistry*, edited by H. Yersin (Springer, Berlin, 2001), p. 213.

[23] G. Chen, R. G. Haire, and J. R. Peterson, Appl. Spectrosc. **46**, 1495 (1992).

[24] A. Grzechnik, K. Syassen, I. Loa, M. Hanfland, and J. Y. Gesland, Phys. Rev. B **65**, 104102 (2002).

[25] K. W. H. Stevens, Proc. Phys. Soc., London, Sect. A **65**, 149 (1952).

[26] G. H. Dieke, in *Spectra and Energy Levels of Rare Earth Ions in Crystals*, edited by H. M. Crosswhite and H. Crosswhite (Wiley, New York, 1968).

[27] D. J. Newman and B. Ng, Rep. Prog. Phys. **52**, 699 (1989).

[28] Th. Tröster, T. Gregorian, and W. B. Holzapfel, Phys. Rev. B **48**, 2960 (1993).

[29] C. Bungenstock, Th. Tröster, and W. B. Holzapfel, Phys. Rev. B **62**, 7945 (2000).

[30] I. Loa, M. Divis, V. Nekvasil, S. Jandl, K. Syassen, A. A. Nugroho, and A. A. Menovsky, Phys. Rev. B **64**, 214106 (2001).

[31] N. C. Chang, J. B. Gruber, R. P. Leavitt, and C. A. Morrison, J. Chem. Phys. **76**, 3877 (1982).

[32] O. Guillot-Noël, B. Viana, G. Aka, A. Kahn-Harari, D. Gourier, and D. Vivien, J. Lumin. **72-74**, 195 (1997).

[33] H. Pascard, Phys. Rev. B **31**, 2925 (1985).

[34] E. Antic-Fidancev, J. Hölsä, M. Lastusaari, and A. Lupei, Phys. Rev. B **64**, 195108 (2001).

[35] F. S. Ermeneux, C. Goutaudier, R. Moncorgé, M. T. Cohen-Adad, M. Bettinelli, and E. Cavalli, Opt. Mater. (Amsterdam, Neth.) **13**, 193 (1999).